Applied Numerical Mathematics 106 (2016) 37–52

Contents lists available at ScienceDirect

Applied Numerical Mathematics

www.elsevier.com/locate/apnum

On the robustness of ILU smoothers on triangular grids

M.A.V. Pinto [a], C. Rodrigo [b,*], F.J. Gaspar [c], C.W. Oosterlee [d,e]

[a] Department of Mechanical Engineering, Federal University of Paraná (UFPR), Curitiba, PR, Brazil
[b] Department of Applied Mathematics, University of Zaragoza, María de Luna 3, 50018, Zaragoza, Spain
[c] Department of Applied Mathematics, University of Zaragoza, Pedro Cerbuna 9, 50012, Zaragoza, Spain
[d] CWI, Centrum Wiskunde & Informatica, Science Park 123, 1098 XG Amsterdam, The Netherlands
[e] Delft University of Technology, The Netherlands

ARTICLE INFO

Article history:
Received 10 August 2015
Received in revised form 21 January 2016
Accepted 5 February 2016
Available online 22 March 2016

Keywords:
Multigrid
Incomplete factorization
ILU smoother
Local Fourier analysis

ABSTRACT

In this work, incomplete factorization techniques are used as smoothers within a geometric multigrid algorithm on triangular grids. A local Fourier analysis is proposed to study the smoothing properties of these methods, as well as the asymptotic convergence of the whole multigrid procedure. With this purpose, two- and three-grid local Fourier analysis are performed. Several two-dimensional diffusion problems, including different kinds of anisotropy are considered to demonstrate the robustness of this type of methods.

1. Introduction

The solution of large sparse algebraic systems of equations is of great interest due to the wide range of applications in which they are involved, as they occur for example in the numerical solution of partial differential equations. Since the factor matrices L and U do not have a sparse structure anymore, to compute the exact LU factorization of a large but sparse $n \times n$ regular matrix $\mathcal{O}(n^3)$ arithmetic operations are needed, which is not practicable for large values of n. Incomplete factorization methods can be seen as approximation of the exact LU factorization of a matrix A in which fill-ins are allowed only at a restricted set of positions in the LU factors, in order to ensure that the action of A^{-1} is inexpensive. These iterative methods can be applied to any sparse matrix in principle and they are often very robust with respect to anisotropic coefficients for example.

The class of incomplete factorization methods was first introduced in [5,19,20] as methods for solving discretizations of PDEs. However, they can be seen in a more general way as matrix splitting techniques, see [28,29]. Furthermore, since Evans in [8] proposed the use of sparse LU factors as preconditioners, these methods have been successfully applied as preconditioners for linear systems. Meijerink and Van der Vorst [17] proved the existence of incomplete LU (ILU) preconditioners for M-matrices, and Gustafsson [10] modifies the incomplete factorization preconditioner in order to obtain improved spectral properties. A good introduction to these methods can be found in the books by Hackbusch [12] and Axelsson [2], and in the overview papers [1,7], for example. Finally, in [13], a collection of research papers related to incomplete decompositions is presented.

* Corresponding author.
E-mail addresses: marcio_villela@ufpr.br (M.A.V. Pinto), carmenr@unizar.es (C. Rodrigo), fjgaspar@unizar.es (F.J. Gaspar), c.w.oosterlee@cwi.nl (C.W. Oosterlee).
URLs: http://www.unizar.es/pde/fjgaspar/index.html (F.J. Gaspar), http://www.ta.twi.tudelft.nl/mf/users/oosterle (C.W. Oosterlee).

http://dx.doi.org/10.1016/j.apnum.2016.02.007
0168-9274/

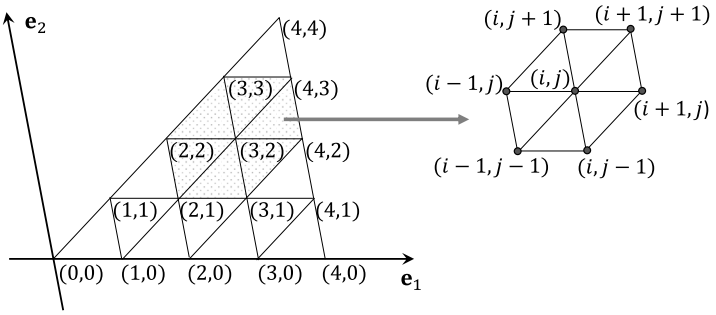

Fig. 1. New basis in $\mathbb{R}^2$ fitting the geometry of the triangular grid, local numbering of the regular grid obtained after two refinement levels and numbering for the stencil operator.

Multigrid methods [11,25,26,31] aim at improving the convergence of classical iterative methods for solving large sparse systems of algebraic equations. They are among the fastest solvers for this kind of problems. However, they strongly depend on the so-called components of the algorithm. In geometric multigrid, usually the most influent component is the relaxation procedure. ILU decompositions were introduced as smoothers in the multigrid technique by Wesseling et al. (see [30,32]), and since then, they were often used as smoothers for different applications (see [15,24,35,36], for example). Also, a modified ILU smoother was proposed in [16,18,23,36], which has favorable properties for dealing with anisotropic problems. In particular, G. Wittum [36] was the first to rigorously prove the robustness of this smoother for an anisotropic model problem, and R. Stevenson [23] generalized the results in [36]. More recently, in [27], a fast preconditioner solver based on multigrid with an ILU smoother was proposed for solving heterogeneous high-wavenumber Helmholtz problems, and in [21], a new relaxation methodology based on a truncated ILU smoother is presented for multigrid preconditioning of discrete convection–diffusion problems.

Local Fourier analysis (LFA) [3,4,33] deals with the quantitative analysis of geometric multigrid methods. It is used to analyze the smoothing properties of the relaxation procedures or/and the asymptotic convergence of the two-, three-, ..., k-grid methods. LFA provides very accurate predictions of the asymptotic convergence factors of these algorithms for many problems, especially for elliptic problems, and for this reason it becomes a very practical tool for the design of suitable multigrid components for different problems. This analysis assumes some simplifications: boundary conditions are neglected by formally defining the discrete operator, which must be given by a constant stencil, on an infinite regular grid. Regarding the application of LFA for the study of incomplete factorization techniques, one of these assumptions is not satisfied, since near the boundaries of the domain the stencils involved in the decomposition vary. However, they tend rapidly to constant stencils away from the boundaries and therefore local Fourier analysis is able to provide useful predictions also for this type of methods. For example, its usefulness is proven in [31], where a smoothing analysis for a wide variety of incomplete factorization methods applied to different problems on rectangular grids was performed. Smoothing properties of ILU-type smoothers on rectangular grids were studied in [6,15,35,36], for example. However, the analysis of these relaxation processes on triangular grids, as well as a more detailed study of the multigrid convergence (two-, three- or k-grid analysis) is missing in the literature. Therefore, in this work, we want to close this gap in order to provide a tool to study these methods in a more flexible framework.

The remainder of the paper is organized as follows. In Section 2, the considered incomplete factorization techniques on triangular grids are introduced. Section 3 shows how to perform a local Fourier analysis for multigrid based on ILU smoothers. Smoothing as well as two- and three-grid analysis are described. In Section 4, local Fourier analysis results are displayed for different two-dimensional diffusion equations, including also anisotropic problems. In this section, we demonstrate the sharpness of the proposed LFA, showing a very accurate match between theoretical and experimentally computed convergence factors. Finally, in Section 5, we present two numerical experiments to show on the one hand the suitability of ILU smoothers for some anisotropic problems and on the other hand to illustrate the usefulness of the LFA to build block-wise multigrid methods on semi-structured triangular grids.

2. Incomplete decomposition techniques for structured triangular grids

We are interested in the study of incomplete decomposition techniques for symmetric matrices arising from the discretization of partial differential equations on structured triangular grids. These meshes arise from the application of a regular refinement process to a triangle, that is, the regular triangular grid is constructed by dividing the triangle into four congruent triangles connecting the midpoints of the edges, and so forth until the mesh has the desired fine scale to approximate the solution of the problem. In this way, for a fixed number of refinement steps ℓ, we can define the regular grid arising inside the triangle as follows

$$G_\ell = \{\mathbf{x} = (x, y)|_{\{\mathbf{e}_1, \mathbf{e}_2\}} \mid x = k_x h_x,\ y = k_y h_y,\ k_x = 0, \ldots, 2^\ell,\ k_y = 0, \ldots, k_x\}, \tag{2.1}$$

where $\{\mathbf{e}_1, \mathbf{e}_2\}$ are unit vectors defining a coordinate system in $\mathbb{R}^2$ fitting the geometry of the triangular grid, and h_x and h_y are the grid spacings associated with the refinement level ℓ. $(x, y)|_{\{\mathbf{e}_1,\mathbf{e}_2\}}$ denotes the coordinates of $\mathbf{x}$ in the new coordinate system. (k_x, k_y) provides a double index local numbering (see left part of Fig. 1) very convenient for identifying the neighboring nodes and for defining the stencil form of the sparse matrix under consideration. We will focus on discretizations based on a 7-point stencil (see Fig. 1) that, for a grid point (i, j), can be represented as follows

$$A^{ij} = \begin{bmatrix} \cdot & a_{i,j+1} & a_{i+1,j+1} \\ a_{i-1,j} & a_{i,j} & a_{i+1,j} \\ a_{i-1,j-1} & a_{i,j-1} & \cdot \end{bmatrix}. \tag{2.2}$$

The standard incomplete decomposition for a symmetric matrix A is given by a splitting $A = M - R$, where R is the so-called rest matrix and

$$M = (L + D)D^{-1}(L^T + D)$$

with D a diagonal matrix and L a strictly lower triangular matrix. This splitting defines an iterative method

$$(L + D)D^{-1}(L^T + D)u^{m+1} = f + Ru^m, \tag{2.3}$$

with iteration matrix $(I - M^{-1}A) = (I - (L^T + D)^{-1}D(L + D)^{-1}A)$.

This kind of iterations can also be expressed in stencil form by replacing the matrix notation in (2.3) by the corresponding stencil operators. If a 7-point incomplete decomposition with respect to a west-to-east, south-to-north lexicographical ordering of the grid points is considered, the following stencil operators have to be considered, according to the numbering in Fig. 1,

$$L^{ij} = \begin{bmatrix} \cdot & \cdot & \cdot \\ l_{i-1,j} & \cdot & \cdot \\ l_{i-1,j-1} & l_{i,j-1} & \cdot \end{bmatrix}, \qquad D^{ij} = \begin{bmatrix} \cdot & \cdot & \cdot \\ \cdot & d_{i,j} & \cdot \\ \cdot & \cdot & \cdot \end{bmatrix}, \qquad R^{ij} = \begin{bmatrix} r_{i-1,j+1} & \cdot & \cdot \\ \cdot & \cdot & \cdot \\ \cdot & \cdot & r_{i+1,j-1} \end{bmatrix}. \tag{2.4}$$

Although several orderings can be considered to define different ILU decompositions, in the rest of this work this ordering will be mainly considered.

Usually a *modified incomplete factorization*, ILU_σ is considered [16,18,36,23]. This ILU_σ-decomposition of a symmetric matrix A is given by

$$A = (L + D_\sigma)D_\sigma^{-1}(L^T + D_\sigma) - R_\sigma,$$

where $D_\sigma = D + \sigma\widetilde{D}$, with a diagonal matrix $\widetilde{D}$ where each diagonal element is given by $\widetilde{d}_{ii} = \sum_{j\neq i} |r_{ij}^\sigma|$. From now on, we will consider ILU_σ but we will refer to $R_\sigma = (r_{ij}^\sigma)$ as $R = (r_{ij})$ for simplicity in the notation.

Notice that the iteration matrix of the incomplete decomposition iteration can be also written in terms of matrices A and R as follows

$$(I - M^{-1}A) = (I - (A + R)^{-1}A) = (A + R)^{-1}R. \tag{2.5}$$

This expression will be considered for the computation of the Fourier symbols in the local Fourier analysis.

3. One-, two- and three-grid local Fourier analysis for multigrid based on ILU smoothers

Local Fourier analysis is a technique based on the Discrete Fourier Transform. Some reasonable assumptions have to be done to perform this analysis; an infinite regular grid is considered, where formally the discrete operator is defined by a constant coefficient stencil, and boundary conditions are not taken into account.

3.1. Notation and basics of LFA for ILU smoothers

The application of this analysis in order to study the smoothing properties of the ILU relaxation is not straightforward. A has to be represented by a constant discretization stencil. However, for ILU smoothing, this is not the case for L, U and R, since the decomposition of A varies near the boundaries. Nevertheless, the representation of A tends to a constant stencil away from the boundaries, and local Fourier analysis can be performed by using these limit stencils. This fact has to be considered in the analysis for this kind of relaxation.

Since we are working on triangular grids, the ideas about the recently introduced LFA on triangular meshes [9,22] have to be taken into account. The key fact for this extension is to consider an expression of the Fourier transform in new coordinate systems in space and frequency variables. To this purpose, we establish a non-orthogonal unit basis of $\mathbb{R}^2$, $\{\mathbf{e}_1, \mathbf{e}_2\}$, which is chosen fitting the geometry of the given mesh, as seen in Fig. 2, and the basis corresponding to the frequencies space, $\{\mathbf{e}'_1, \mathbf{e}'_2\}$, is taken as its dual basis, see Fig. 2; that is, the vectors of the bases satisfy $(\mathbf{e}_i, \mathbf{e}'_j) = \delta_{ij}$, $1 \leq i, j \leq 2$. From the obtained Fourier inversion formula, any discrete function can be written as a formal linear combination of discrete exponential functions of the form

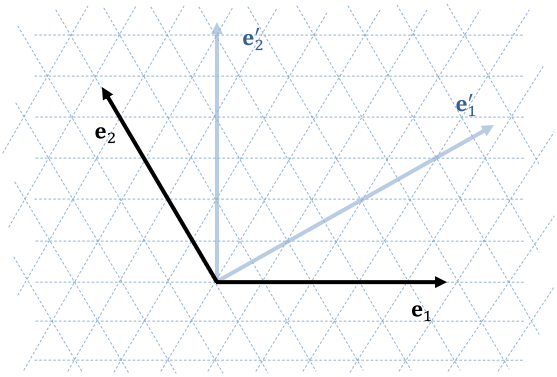

Fig. 2. $\{\mathbf{e}_1, \mathbf{e}_2\}$ non-orthogonal basis on $\mathbb{R}^2$, and its dual basis $\{\mathbf{e}_1', \mathbf{e}_2'\}$.

$$\varphi_h(\boldsymbol{\theta}, \mathbf{x}) = e^{\imath \boldsymbol{\theta}\cdot\mathbf{x}} = e^{\imath\theta_1 x_1} e^{\imath\theta_2 x_2}, \quad \boldsymbol{\theta} \in \Theta_h = (-\pi, \pi] \times (-\pi, \pi].$$

In order to perform the local Fourier analysis for the ILU-type methods, it is well-known (see [31]) that one has to compute the corresponding decomposition on an infinite grid, where the stencils given in (2.4) do not depend on (i, j) anymore. This implies that we have to compute the coefficients from the following equality,

$$\begin{bmatrix} \cdot & a_{0,-1} & a_{-1,-1} \\ a_{-1,0} & a_{0,0} & a_{-1,0} \\ a_{-1,-1} & a_{0,-1} & \cdot \end{bmatrix} = \begin{bmatrix} \cdot & \cdot & \cdot \\ l_{-1,0} & d_{0,0} & \cdot \\ l_{-1,-1} & l_{0,-1} & \cdot \end{bmatrix} \begin{bmatrix} \cdot & \cdot & \cdot \\ \cdot & d_{0,0}^{-1} & \cdot \\ \cdot & \cdot & \cdot \end{bmatrix} \begin{bmatrix} \cdot & l_{0,-1} & l_{-1,-1} \\ \cdot & d_{0,0} & l_{-1,0} \\ \cdot & \cdot & \cdot \end{bmatrix} - \begin{bmatrix} r_{1,-1} & \cdot & \cdot \\ \cdot & 2\sigma|r_{1,-1}| & \cdot \\ \cdot & \cdot & r_{1,-1} \end{bmatrix}. \tag{3.1}$$

Therefore, we obtain the following non-linear system of equations,

$$\begin{aligned} a_{-1,-1} &= l_{-1,-1}, \\ a_{0,-1} &= \frac{l_{-1,-1}}{d_{0,0}} l_{-1,0} + l_{0,-1}, \\ a_{-1,0} &= \frac{l_{-1,-1}}{d_{0,0}} l_{0,-1} + l_{-1,0}, \\ a_{0,0} &= \frac{l_{-1,-1}^2}{d_{0,0}} + \frac{l_{-1,0}^2}{d_{0,0}} + \frac{l_{0,-1}^2}{d_{0,0}} + d_{0,0} - 2\sigma|r_{1,-1}|, \\ 0 &= \frac{l_{-1,0}}{d_{0,0}} l_{0,-1} - r_{1,-1}. \end{aligned} \tag{3.2}$$

As an example, we consider the case of ILU$_\sigma$ relaxation with $\sigma = 1$ for the Laplace operator discretized by linear finite elements on an equilateral triangular grid, which is given by the following stencil form,

$$A = \begin{bmatrix} \cdot & -2/3 & -2/3 \\ -2/3 & 4 & -2/3 \\ -2/3 & -2/3 & \cdot \end{bmatrix}. \tag{3.3}$$

Taking into account that $a_{0,-1} = a_{-1,0}$ implies $l_{0,-1} = l_{-1,0}$, as can be easily seen, system (3.2) is reduced to

$$\begin{aligned} l_{-1,-1} &= -2/3, \\ -2/3 &= \frac{l_{-1,-1}}{d_{0,0}} l_{-1,0} + l_{-1,0}, \\ 4 &= \frac{l_{-1,-1}^2}{d_{0,0}} + d_{0,0}, \\ 0 &= \frac{l_{-1,0}^2}{d_{0,0}} - r_{1,-1}. \end{aligned} \tag{3.4}$$

Notice that this system can be easily solved by first obtaining $d_{0,0}$ from the third equation and substituting this value to obtain the rest of unknowns, $l_{-1,0}$ and $r_{1,-1}$. The resulting decomposition is given by

$$L+D=\frac{1}{3}\begin{bmatrix} \cdot & \cdot & \cdot \\ \dfrac{-3-2\sqrt{2}}{1+\sqrt{2}} & 6+4\sqrt{2} & \cdot \\ -2 & \dfrac{-3-2\sqrt{2}}{1+\sqrt{2}} & \cdot \end{bmatrix},\ R=\frac{1}{6}\begin{bmatrix} 1 & \cdot & \cdot \\ \cdot & 2 & \cdot \\ \cdot & \cdot & 1 \end{bmatrix}. \tag{3.5}$$

In the general case, the solution of system (3.2) can be computed, taking into account that $l_{-1,-1}=a_{-1,-1}$, by the following recursion process.

Given

$$d^0_{0,0}=a_{0,0},\ l^0_{-1,0}=a_{-1,0},\ l^0_{0,-1}=a_{0,-1},\ r^0_{1,-1}=\frac{l^0_{-1,0}}{d^0_{0,0}}l^0_{0,-1}$$

Compute for $k=1,\ldots$

$$l^k_{0,-1}=a_{0,-1}-\frac{l_{-1,-1}}{d^{k-1}_{0,0}}l^{k-1}_{-1,0},$$

$$l^k_{-1,0}=a_{-1,0}-\frac{l_{-1,-1}}{d^{k-1}_{0,0}}l^k_{0,-1},$$

$$d^k_{0,0}=\frac{-1}{d^{k-1}_{0,0}}\left(l^2_{-1,-1}+(l^k_{-1,0})^2+(l^k_{0,-1})^2\right)+a_{0,0}+2\sigma|r^{k-1}_{1,-1}|,$$

$$r^k_{1,-1}=\frac{l^k_{-1,0}}{d^k_{0,0}}l^k_{0,-1}. \tag{3.6}$$

Once system (3.2) is solved and we have the decomposition corresponding to the ILU$_\sigma$ algorithm, we can write the iteration matrix only in terms of entries of A and R as in (2.5).

3.2. Smoothing analysis

The Fourier symbol of the ILU$_\sigma$ iteration matrix, that is, the representation of such operator on the Fourier space, is easily computed by the following expression

$$\widetilde{S}(\boldsymbol{\theta})=\frac{\widetilde{R}(\boldsymbol{\theta})}{\widetilde{A}(\boldsymbol{\theta})+\widetilde{R}(\boldsymbol{\theta})}. \tag{3.7}$$

To obtain convergence of the method, $|\widetilde{S}(\boldsymbol{\theta})|$ should be strictly less than one for each $\boldsymbol{\theta}\in\Theta_h$. However, since we are interested in using ILU$_\sigma$ as smoother in a multigrid procedure, it suffices to study its smoothing property, that is, the way in which such relaxation annihilates the high-frequency components of the error (the components associated with the frequencies $\boldsymbol{\theta}\in\Theta_h\setminus\Theta_{2h}$, where $\Theta_{2h}=(-\pi/2,\pi/2]\times(-\pi/2,\pi/2]$). This property is given by the so-called smoothing factor, defined as follows,

$$\mu=\sup_{\boldsymbol{\theta}\in\Theta_h\setminus\Theta_{2h}}|\widetilde{S}(\boldsymbol{\theta})|. \tag{3.8}$$

In order to illustrate this analysis, we can easily compute the Fourier symbol of the iteration matrix in the previous example (Laplace operator on the equilateral triangular grid). This will be fully determined by the corresponding Fourier symbols of R and A:

$$\widetilde{R}(\boldsymbol{\theta})=\frac{1}{3}\left(1+\cos(\theta_1-\theta_2)\right), \tag{3.9}$$

$$\widetilde{A}(\boldsymbol{\theta})=4\left(1-\frac{1}{3}\cos(\theta_1)-\frac{1}{3}\cos(\theta_2)-\frac{1}{3}\cos(\theta_1+\theta_2)\right). \tag{3.10}$$

From this symbol and by using definition (3.8), we can numerically approximate the smoothing factor of this relaxation method by considering a very fine grid in the frequency space. The resulting value is $\mu\approx 0.125$, and in Fig. 3 we can observe the amplification factors for each pair of frequencies of the grid. Notice that, although all frequencies in Θ_h are displayed in the picture, we are only interested in the values of the subset $\Theta_h\setminus\Theta_{2h}$.

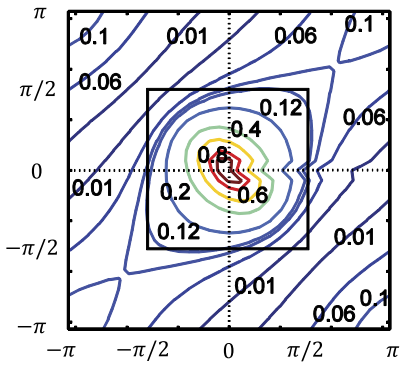

Fig. 3. Reduction factors of Fourier components for ILU_1.

3.3. Two-grid analysis

In order to investigate the interplay between relaxation and coarse-grid correction, which is crucial for an efficient multigrid method, it is necessary to perform at least a two-grid analysis which takes into account the effect of transfer operators. For this purpose, one needs to consider the error propagation operator from the two-grid method, that is,

$$M_h^{2h} = S_h^{\nu_2}(I_h - I_{2h}^h A_{2h}^{-1} I_h^{2h} A_h) S_h^{\nu_1},$$

where S_h is the smoothing procedure, ν_1 and ν_2 are the number of pre- and post-smoothing steps respectively, and the coarse-grid correction operator is composed of the discrete operators on the fine and coarse grids, A_h and A_{2h}, respectively, and the inter-grid transfer operators: restriction, I_h^{2h} and prolongation I_{2h}^h. Notice that here h and $2h$ refer to two consecutive fine and coarse grids, where the first one is obtained from the latter by applying a regular refinement process. The two-grid analysis is the basis for the classical asymptotic multigrid convergence estimates, and the spectral radius of the two-grid operator, $\rho(M_h^{2h})$, indicates the asymptotic convergence factor of the two-grid method. To estimate this value, the crucial observation is that the coarse-grid correction operator, as well as the smoother, leave the so-called spaces of $2h$-harmonics, $\mathcal{F}^4(\boldsymbol{\theta}^{00})$, invariant. These subspaces are given by

$$\mathcal{F}^4(\boldsymbol{\theta}^{00}) = span\{\phi_h(\boldsymbol{\theta}^{\alpha_1\alpha_2}, \mathbf{x}) | \alpha_1, \alpha_2 \in \{0, 1\}\}, \text{ with } \boldsymbol{\theta}^{00} \in (-\pi/2, \pi/2]^2,$$

and where $\boldsymbol{\theta}^{\alpha_1\alpha_2} = \boldsymbol{\theta}^{00} - (\alpha_1 \mathrm{sign}(\theta_1^{00})\pi, \alpha_2 \mathrm{sign}(\theta_2^{00})\pi)$. For this reason, M_h^{2h} is equivalent to a block-diagonal matrix consisting of blocks denoted by $\widetilde{M}_h^{2h}(\boldsymbol{\theta}^{00}) = M_h^{2h}|_{\mathcal{F}^4(\boldsymbol{\theta}^{00})}$, that is, its Fourier domain representation. In this way, one can determine the spectral radius $\rho(M_h^{2h})$ by calculating the spectral radius of these smaller matrices, that is:

$$\rho_{2g} = \rho(M_h^{2h}) = \sup_{\boldsymbol{\theta}^{00} \in (-\pi/2, \pi/2]^2} \rho(\widetilde{M}_h^{2h}(\boldsymbol{\theta}^{00})). \tag{3.11}$$

3.4. K-grid analysis

A deeper insight into the performance of multigrid can be obtained by considering a k-grid analysis ($k > 2$). For example, the influence of the type of cycle (V-cycle versus W-cycle) and/or the number of pre- and post-smoothing steps cannot be accurately predicted by a classical Fourier two-grid analysis. Due to the recursive definition of the k-grid operator, the previously introduced two-grid analysis can be extended to a k-grid analysis, and in particular to a three-grid analysis [34]. Analogously to the case of the two-grid cycle, the expression giving the transformation of the error by a three-grid cycle is $e_h^{m+1} = M_h^{4h} e_h^m$, with

$$M_h^{4h} = S_h^{\nu_2} C_h^{4h} S_h^{\nu_1} = S_h^{\nu_2}(I_h - I_{2h}^h (I_{2h} - (M_{2h}^{4h})^\gamma)(A_{2h})^{-1} I_h^{2h} A_h) S_h^{\nu_1},$$

being M_{2h}^{4h} the two-grid operator between the two coarse grids, defined as

$$M_{2h}^{4h} = S_{2h}^{\nu_2}(I_{2h} - I_{4h}^{2h}(A_{4h})^{-1} I_{2h}^{4h} A_{2h}) S_{2h}^{\nu_1},$$

and γ the number of two-grid iterations. Similarly to the decomposition of the Fourier space into the subspaces of $2h$-harmonics in the two-grid analysis, for the three-grid analysis it has to be taken into account that not only in the transition from the finest to the second grid but also in the transition from the second grid to the coarsest grid four frequencies are coupled. Taking this into account, we can define appropriate subspaces of $4h$-harmonics, generated for the Fourier components associated with the sixteen frequencies coupled on the coarsest grid

$$\mathcal{F}^{16}(\boldsymbol{\theta}^{00}) = span\{\varphi_h(\boldsymbol{\theta}_{nm}^{ij}),\ i, j, n, m \in \{0, 1\}\}, \tag{3.12}$$

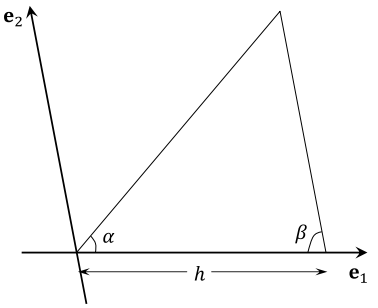

Fig. 4. Triangular domain characterized by angles α and β and length h.

with $\boldsymbol{\theta}^{00} = (\theta_1^{00}, \theta_2^{00}) \in \boldsymbol{\Theta}_{4h} = (-\pi/4, \pi/4] \times (-\pi/4, \pi/4]$, and where

$$\boldsymbol{\theta}_{nm}^{00} = \boldsymbol{\theta}^{00} - (n\pi\ sign(\theta_1^{00})/2, m\pi\ sign(\theta_2^{00})/2), \tag{3.13}$$

$$\boldsymbol{\theta}_{nm}^{ij} = \boldsymbol{\theta}_{nm}^{00} - (i\pi\ sign((\theta_{nm}^{00})_1), j\pi\ sign((\theta_{nm}^{00})_2)), \tag{3.14}$$

being $i, j, n, m \in \{0, 1\}$. Then, by denoting as $\widetilde{M}_h^{4h}(\boldsymbol{\theta}^{00})$ the block-matrix representation of M_h^{4h} on the Fourier space, the asymptotic three-grid convergence factor can be computed as the supreme of the spectral radii of the corresponding blocks

$$\rho_{3g} = \rho(M_h^{4h}) := \sup_{\boldsymbol{\theta}^{00} \in \boldsymbol{\Theta}_{4h}} \rho(\widetilde{M}_h^{4h}(\boldsymbol{\theta}^{00})). \tag{3.15}$$

In order to illustrate the suitability of the presented local Fourier analysis, next sections are devoted to present some LFA results and to illustrate their usefulness.

4. Local Fourier analysis results

In order to validate the theoretical analysis presented in Section 3, we consider the following two-dimensional diffusion equation

$$\nabla \cdot (K \nabla u(\mathbf{x})) = f(\mathbf{x}),\ \mathbf{x} \in \Omega, \tag{4.1}$$

where $K = \begin{pmatrix} k_{11} & k_{12} \\ k_{12} & k_{22} \end{pmatrix}$ is a symmetric and positive definite diffusion tensor. Throughout this section, Ω will denote a triangular domain characterized by two angles α and β and the length h of its base, which is assumed to be parallel to the x-coordinate axis (see Fig. 4). We discretize problem (4.1) by linear finite element methods on the target triangular grid arising from several refinement levels of Ω. The resulting operator in stencil form can be written as a function of the geometric parameters defining the geometry as follows

$$\begin{aligned} A_h = \frac{k_{11}}{h^2}\begin{bmatrix} 0 & 0 & 0 \\ -1 & 2 & -1 \\ 0 & 0 & 0 \end{bmatrix} + \frac{k_{12}}{h^2}\begin{bmatrix} 0 & ca+cb & -ca-cb \\ ca-cb & -2(ca-cb) & ca-cb \\ -ca-cb & ca+cb & 0 \end{bmatrix} \\ + \frac{k_{22}}{h^2}\begin{bmatrix} 0 & -ca^2-ca\,cb & -cb^2-ca\,cb \\ ca\,cb & 2(ca^2+cb^2+ca\,cb) & ca\,cb \\ -cb^2-ca\,cb & -ca^2-ca\,cb & 0 \end{bmatrix}, \end{aligned} \tag{4.2}$$

where $ca = \cot(\alpha)$ and $cb = \cot(\beta)$.

Notice that for this problem, it is difficult to deduce the direction of the possible anisotropy introduced by the tensor definition, and therefore, it is no longer possible to choose a grid oriented with the direction of such an anisotropy. As a consequence, a robust smoother has to be used and we are going to confirm that this is the case of the ILU smoother.

Next, we present results of the local Fourier analysis previously introduced for the ILU smoother for three different choices of tensor K. For this purpose, we assume that the rest of the multigrid components are the standard ones. That is, we consider the canonical interpolation and restriction for linear finite elements, and direct discretization on the coarse grids.

4.1. Laplace equation, $K = I$

First choice of K is corresponding to the Laplace operator. For the following results, we consider the ILU_σ smoother with $\sigma = 1$. In order to see the agreement between the LFA results and those experimentally computed, we have chosen three representative triangular domains: an equilateral triangle, an isosceles right triangle and an isosceles triangle with

Table 1
Smoothing and two-grid convergence factors predicted by LFA together with the experimentally computed asymptotic convergence factor for three representative triangular domains and for different numbers of smoothing steps.

ν	Equilateral			Right triangle			Isosceles ($\alpha = \beta = 80°$)		
	μ^ν	ρ_{2g}	ρ_h	μ^ν	ρ_{2g}	ρ_h	μ^ν	ρ_{2g}	ρ_h
1	0.125	0.126	0.125	0.086	0.119	0.118	0.306	0.303	0.302
2	0.016	0.034	0.033	0.007	0.045	0.044	0.094	0.093	0.093
3	0.002	0.019	0.019	6.3e–04	0.029	0.028	0.029	0.057	0.057
4	2.4e–04	0.013	0.013	5.4e–05	0.022	0.021	0.009	0.042	0.042

Table 2
Two-grid convergence factors predicted by LFA, using the ILU_1 smoother with $\sigma = 1$ with two smoothing steps for different triangles in function of two of their angles.

α/β	10	20	30	40	50	60	70	80	90
10	0.098	0.097	0.096	0.096	0.097	0.099	0.103	0.124	0.176
20	0.088	0.084	0.082	0.079	0.078	0.077	0.078	0.093	0.137
30	0.075	0.071	0.067	0.064	0.062	0.059	0.060	0.088	0.133
40	0.063	0.059	0.055	0.052	0.049	0.047	0.055	0.087	0.133
50	0.052	0.048	0.045	0.042	0.039	0.037	0.055	0.087	0.133
60	0.043	0.040	0.037	0.035	0.033	0.034	0.055	0.087	0.133
70	0.037	0.034	0.032	0.031	0.033	0.037	0.055	0.088	0.137
80	0.032	0.031	0.032	0.035	0.039	0.047	0.060	0.093	0.176
90	0.032	0.034	0.037	0.042	0.049	0.059	0.078	0.124	–

a very small angle (characterized by angles $\alpha = \beta = 80°$). In Table 1, for these three triangular domains we display the smoothing factor, μ^ν, and the two-grid convergence factor, ρ_{2g}, both predicted by the LFA, together with the asymptotic convergence factor experimentally computed by using a W-cycle and a fine-grid obtained after 10-refinement levels, ρ_h. These results are shown for different numbers of smoothing steps $\nu = \nu_1 + \nu_2$, where ν_1 and ν_2 are the numbers of pre- and post-smoothing steps, respectively. From Table 1, we observe that the local Fourier analysis provides very accurate predictions of the experimentally computed asymptotic convergence factors. Moreover, very satisfactory convergence rates, below 0.1, are obtained with only two smoothing steps, which brings us to consider $\nu = 2$ for the rest of experiments carried out in this work. Also it seems that the use of ILU_1 as smoother in the multigrid procedure gives rise to an algorithm that can be robust for different triangulations. This statement is confirmed in Table 2, where the two-grid convergence factor provided by LFA is displayed for a wide range of triangular domains characterized by two of their angles, α and β, see Fig. 4. We observe that a west-to-east and south-to-north lexicographic ordering of the ILU smoother seems to give good results for all triangles, contrary to the behavior of line-smoothers analyzed for example in [22].

Remark 1. In [22], the specific suitable line-smoother depended on the type of grid anisotropy. This was mandatory to obtain satisfactory convergence results. Here, however, it is *not* necessary to choose different orderings of the ILU smoother for any of the triangulations. Furthermore, for non-acute triangulations a linewise smoother that provides satisfactory multigrid convergence factors *does not exist*, whereas the proposed ILU smoother performs well even in these cases. This fact makes the use of ILU as smoother for triangular grids very interesting.

In practice, it is worth to know whether we can use V-cycles instead of W-cycles, due to the high computational cost of the latter. For this purpose, a three-grid analysis, at least, is necessary. Then, in Table 3 we show the three-grid convergence factors predicted by this analysis for both W- and V-cycles, together with the asymptotic convergence factors experimentally obtained (in brackets), for the three representative triangular domains previously considered. These results are presented for different numbers of smoothing steps ν. From the table, we can conclude that V-cycles have better performance than W-cycles since they provide similar convergence factors but V-cycles are cheaper.

4.1.1. σ-dependence

Although throughout all this work we have chosen $\sigma = 1$ for the ILU_σ smoother due to its robustness for all problems considered here, it is worth to mention that for a concrete problem this value of σ does not have to be optimal and we can find other values giving rise to better results. It is clear that local Fourier analysis can help to find the optimal value of σ. To illustrate this, we fix the Laplace problem on the three representative triangular domains previously considered. In Fig. 5(a), we show the two-grid convergence factors predicted by LFA, ρ_{2g} versus various values of σ from 0 to 1.4. From this picture, it is clear that $\sigma = 1$ is not the optimal choice, and that the best one depends on the geometry of the triangular grid. In order to show the influence of parameter σ on the spectrum of the two-grid operator, we display in Fig. 5(b) the corresponding eigenvalues for three different values of σ: $\sigma = 0$ (bottom), $\sigma = 0.5$ (center) and $\sigma = 1$ (top) for the isosceles triangular grid. From these figures, we can observe how the eigenvalues move from left to right, achieving the best location for $\sigma = 0.5$ in this case.

Table 3
Three-grid convergence factors predicted by LFA for W- and V-cycles together with the experimentally computed asymptotic convergence factors (in brackets), for three representative triangular domains and for different numbers of smoothing steps.

Cycle (ν_1, ν_2)	Equilateral	Right triangle	Isosceles
$V(1,0)$	0.135 (0.135)	0.134 (0.133)	0.302 (0.302)
$V(0,1)$	0.135 (0.135)	0.134 (0.134)	0.302 (0.302)
$V(1,1)$	0.042 (0.045)	0.058 (0.061)	0.118 (0.128)
$V(2,0)$	0.042 (0.045)	0.058 (0.061)	0.118 (0.128)
$V(0,2)$	0.042 (0.045)	0.058 (0.061)	0.118 (0.129)
$W(1,0)$	0.126 (0.125)	0.119 (0.118)	0.302 (0.302)
$W(1,1)$	0.034 (0.033)	0.045 (0.045)	0.093 (0.093)

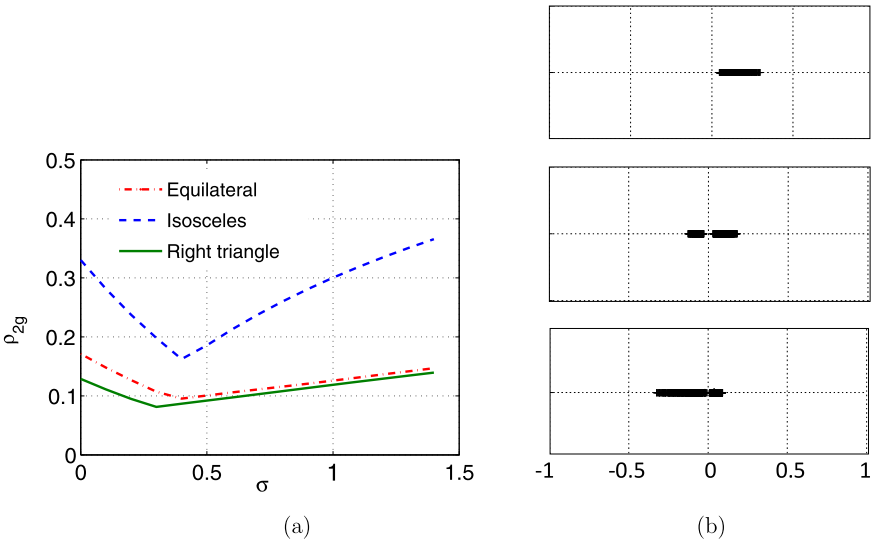

Fig. 5. (a) Two-grid convergence factors predicted by LFA, ρ_{2g} versus various values of σ from 0 to 1.4, for three different triangular grids. (b) Spectrum of the iteration matrix of the two-grid method for three different values of sigma, $\sigma = 0$ (*bottom*), 0.5 (*center*), 1 (*top*), and an isosceles triangular grid with common angle 80°.

4.2. Anisotropic problem

In this section, we consider several anisotropic tensors, characterized by different directions of the anisotropy. First, we analyze the following y-anisotropic tensor

$$K = \begin{pmatrix} 1 & 0 \\ 0 & \varepsilon \end{pmatrix}, \tag{4.3}$$

where ε is a small parameter. This problem is equivalent to analyzing the Laplace problem, as in the previous section, but on an extremely anisotropic grid. We have performed an exhaustive study by using LFA in order to see the robustness of the ILU smoother with respect to the geometry of the grid. In particular, in Table 4, we display the two-grid convergence factors predicted by LFA for a wide range of triangular grids characterized by two of their angles α and β. To obtain these results, $\varepsilon = 10^{-4}$ and two smoothing steps are considered. Moreover, these results have been compared with those experimentally obtained by the real code, showing a very good agreement. For example, in the case of an equilateral triangular grid, the LFA result in the table reads 0.242 and the asymptotic convergence factor experimentally obtained is 0.240; and similar results are obtained for an isosceles triangular grid with common angle 80° where we obtain an experimental convergence factor of around 0.245 which matches very well with 0.247 shown in the table.

Table 4 illustrates the robustness of the multigrid algorithm based on the ILU_1 smoother, since for all possible triangulations, even for obtuse triangular grids, a similar convergence factor around 0.2 is provided. Of course, it is well-known that the convergence properties of incomplete factorization iterations are greatly influenced by the ordering in which the grid-points are updated, and therefore it is possible to consider different orderings that also give rise to very robust smoothers. In fact, a 7-point incomplete decomposition with respect to a south-to-north, east-to-west ordering provides a multigrid convergence factor below 0.03 for any possible configuration.

Next, we analyze the robustness of the proposed method with respect to parameter ε. To this end, in Fig. 6, we show the three-grid convergence factors provided by LFA for different values of ε ranging from 10^{-8} to 1. To obtain these results

Table 4
Two-grid convergence factors predicted by LFA for the y-anisotropic tensor, using ILU_1 smoother with two smoothing steps for different triangles in function of two of their angles.

α/β	10	20	30	40	50	60	70	80	90
10	0.179	0.201	0.209	0.213	0.216	0.218	0.220	0.222	0.223
20	0.189	0.212	0.221	0.226	0.229	0.231	0.233	0.235	0.237
30	0.193	0.217	0.226	0.230	0.234	0.236	0.238	0.240	0.242
40	0.195	0.219	0.228	0.233	0.236	0.239	0.241	0.242	0.244
50	0.196	0.220	0.230	0.234	0.238	0.240	0.242	0.244	0.246
60	0.197	0.222	0.231	0.236	0.239	0.242	0.244	0.245	0.247
70	0.198	0.222	0.232	0.237	0.240	0.243	0.245	0.246	0.248
80	0.199	0.223	0.233	0.238	0.241	0.243	0.246	0.247	0.249
90	0.199	0.224	0.233	0.238	0.242	0.244	0.246	0.248	–

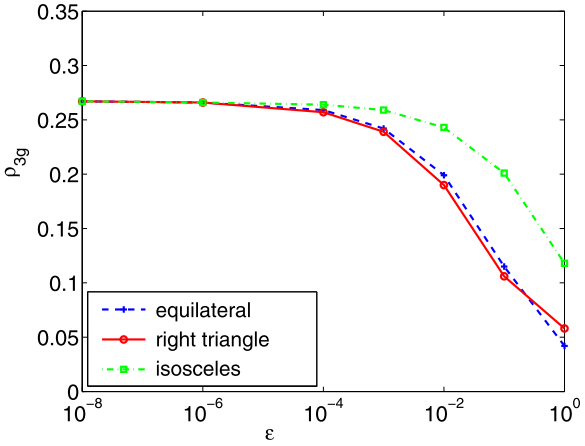

Fig. 6. $V(1,1)$-three-grid convergence factors predicted by LFA, ρ_{3g} for the y-anisotropic tensor, using ILU_1 smoother for three representative triangles.

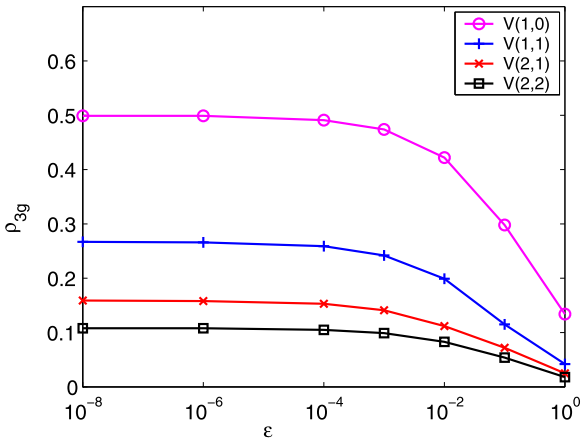

Fig. 7. Three-grid convergence factors predicted by LFA, ρ_{3g} for the y-anisotropic tensor, using ILU_1 smoother for an equilateral triangle and a V-cycle with different numbers of smoothing steps.

a $V(1,1)$-cycle is used and the previous three representative triangles are considered. We can observe from the figure that the proposed algorithm is robust with respect to ε, since when this parameter tends to zero, the three-grid convergence factors remain almost constant around 0.267, independently on the geometry of the three considered triangulations. Notice also that the behavior of the method is very similar for the three triangular grids.

In order to see the influence of the number of smoothing steps, in Fig. 7 we plot the three-grid convergence factors predicted by LFA for different numbers of smoothing steps for an equilateral triangle. We can observe that the three-grid convergence factor obtained by using a V-cycle is robust with respect to the value of ε, independently of the number of smoothing steps that is performed. In fact, even with only one smoothing step, a $V(1,0)$ based on an ILU smoother provides a robust algorithm for an anisotropic problem with small parameter ε.

Table 5
$V(1,1)$-three-grid convergence factors predicted by LFA for the oblique-flow tensor, using the west-to-east and south-to-north ILU_1 smoother with $\gamma = 40°$, $\varepsilon = 10^{-3}$, and two smoothing steps for different triangles in function of two of their angles.

α/β	10	20	30	40	50	60	70	80	90
10	0.0729	0.1185	0.0998	0.1097	0.1359	0.1292	0.1178	0.1363	0.1387
20	0.1283	0.1315	0.1365	0.1310	0.1387	0.1308	0.1389	0.1370	0.1386
30	0.1351	0.1364	0.1360	0.1363	0.1357	0.1352	0.1361	0.1360	0.1358
40	0.0364	0.0367	0.0367	0.0366	0.0366	0.0365	0.0365	0.0365	0.0364
50	0.1325	0.1334	0.1335	0.1340	0.1341	0.1343	0.1343	0.1350	0.1349
60	0.1342	0.1378	0.1363	0.1382	0.1378	0.1360	0.1375	0.1380	0.1388
70	0.1373	0.1362	0.1348	0.1389	0.1382	0.1317	0.1322	0.1352	0.1392
80	0.1299	0.1266	0.1348	0.1344	0.1392	0.1346	0.1352	0.1271	0.1306
90	0.1274	0.1290	0.1283	0.1395	0.1376	0.1038	0.1368	0.1204	–

4.3. Rotated anisotropic problem

Next, we consider a homogeneous full-tensor which represents an anisotropy in the direction at γ degrees from the horizontal,

$$K = R_\gamma \begin{pmatrix} 1 & 0 \\ 0 & \varepsilon \end{pmatrix} R_\gamma^{-1}, \tag{4.4}$$

where R_γ is the rotation of angle γ. Notice that this experiment would be equivalent to solving the anisotropic problem in the previous section on a rotated triangular domain.

First, we fix the values $\gamma = 40°$ and $\varepsilon = 10^{-3}$ and we perform a systematic analysis with respect to the geometry of the grid. More concretely, we want to study for this anisotropic problem the influence of the triangulation on the performance of the ILU smoother within a geometric multigrid method. In Table 5, the three-grid convergence factors predicted by LFA are displayed for a wide range of angles α and β, characterizing the triangular mesh. In these results, a V-cycle with one pre- and one post-smoothing step is considered. We can observe that, for the considered fixed parameters, the multigrid based on the ILU smoother is very robust with respect to the geometry of the triangular grid, since it provides convergence factors always below 0.14 for any combination of angles α and β.

Remark 2. We wish to make a remark about the robustness of the ILU smoother in the case we deal with a fixed direction of the anisotropy. Linewise smoothers do not give satisfactory convergence results for different geometries and a fixed angle γ. If a three-grid local Fourier analysis is performed with linewise smoothing, we observe that only satisfactory $V(1,1)$-convergence factors are obtained when $\alpha = \gamma$, that is, when the anisotropy is aligned with the grid. More concretely, a factor of around 0.13 is obtained in this case, whereas for other geometries the provided convergence factors are around 0.8. Therefore, the use of ILU smoothers for this type of problem is highly advantageous compared to the application of linewise smoothers.

The robustness of the ILU smoother previously observed is not maintained when angle γ changes. In order to see this behavior, we are going to consider three representative triangles and we analyze the convergence of the $V(1,1)$-cycle for a wide range of anisotropy directions and different values of parameter ε. In Fig. 8 (a), we show the three-grid convergence factors provided by LFA by using ILU smoother in the direction west-to-east, south-to-north. In the radial coordinate we represent the values of ε in a logarithmic scale in $(0,1]$. In the angular coordinate, we vary the direction of the anisotropy from 0° to 360°, counting by tens. In this picture, we can observe that there are some regions for which the predicted convergence factors are not satisfactory when ε becomes smaller. This phenomenon can be observed for example when the direction of the anisotropy is between 60° and 120°. A way to improve the convergence of the multigrid method for these directions of the anisotropy is to consider an ILU smoother with a different ordering. More concretely, if consider the ILU relaxation in the direction south-to-north, east-to-west, we can observe in Fig. 8 (b) that the convergence of the V-cycle is good in the range of directions where the previous ILU ordering failed. From this picture we observe that an ILU smoother in the direction south-to-north, east-to-west is not robust regarding the directions of the anisotropy, but both orderings considered are complementary and we can always choose one of these orderings to obtain a satisfactory convergence of the multigrid algorithm. A similar behavior is observed when an isosceles triangular grid with common angle 80° is considered (see Figs. 9(a) and (b)) or for a right triangular grid (see Figs. 10(a) and (b)).

Remark 3. From the results presented in this section, we can conclude that the ILU smoother in the direction west-to-east, south-to-north suffices to provide a robust multigrid algorithm for the solution of the Laplace problem for any regular triangular grid, including any anisotropy of the grid. The same conclusion can be drawn when the anisotropic problem in (4.3) is considered on any triangular grid arising from a triangular domain as in Fig. 4. However, when a rotated anisotropy is induced, the use of local Fourier analysis becomes crucial to determine the ordering of the ILU decomposition that should be selected so that a robust multigrid is obtained.

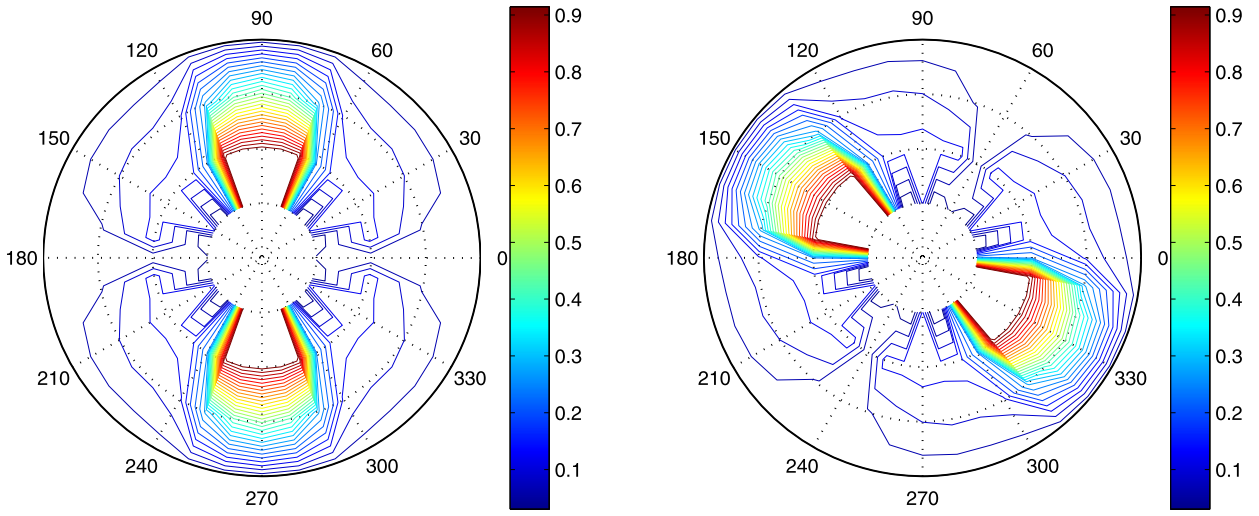

Fig. 8. Three-grid convergence factors predicted by LFA for different values of ε (radial coordinate) and different directions of the anisotropy (angular coordinate) in an equilateral triangular grid, by using a $V(1,1)$-cycle and ILU_1 smoother in the direction (a) west-to-east, south-to-north and (b) south-to-north, east-to-west.

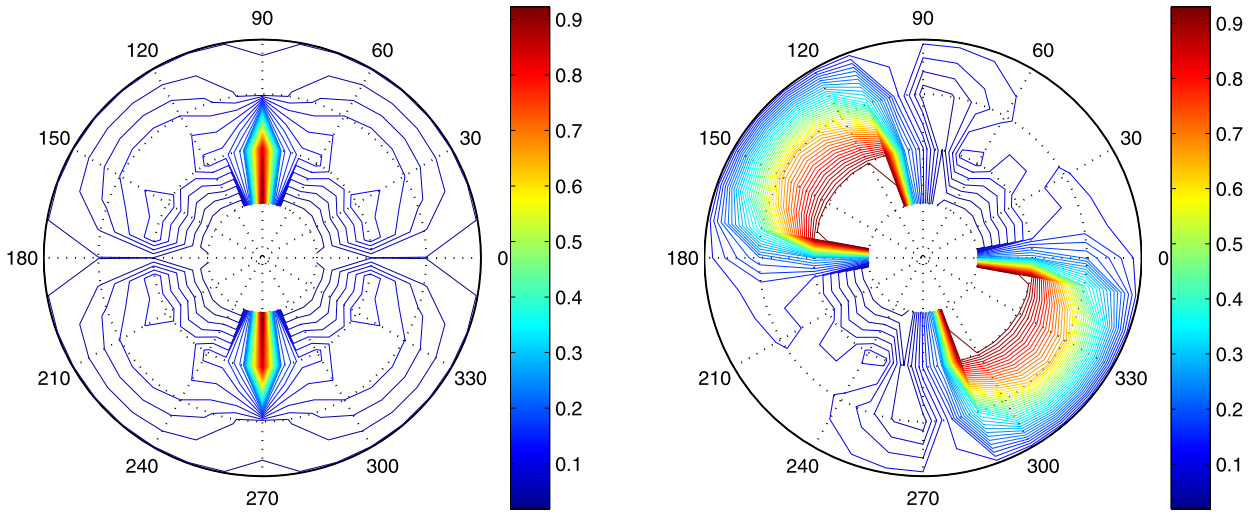

Fig. 9. Three-grid convergence factors predicted by LFA for different values of ε (radial coordinate) and different directions of the anisotropy (angular coordinate) in an isosceles triangular grid with common angle 80°, by using a $V(1,1)$-cycle and ILU smoother in the direction (a) west-to-east, south-to-north and (b) south-to-north, east-to-west.

Remark 4. The good behavior of ILU smoothers on triangular grids cannot be straightforwardly generalized to three-dimensional tetrahedral grids. More research on this extension is needed, but this topic is out of the scope of this paper.

5. Numerical experiments

In this section, we present two different numerical experiments. The first one deals with the numerical simulation of problem (4.4), considered in Section 4.3, where it is analyzed by using LFA. Here we show how the theoretical results obtained in the previous section are useful to perform real simulations of the problem. In the second numerical experiment, we use the local Fourier analysis performed in this work, to design an efficient geometric multigrid method on semi-structured triangular grids, which are an alternative to solve problems defined in complex domains.

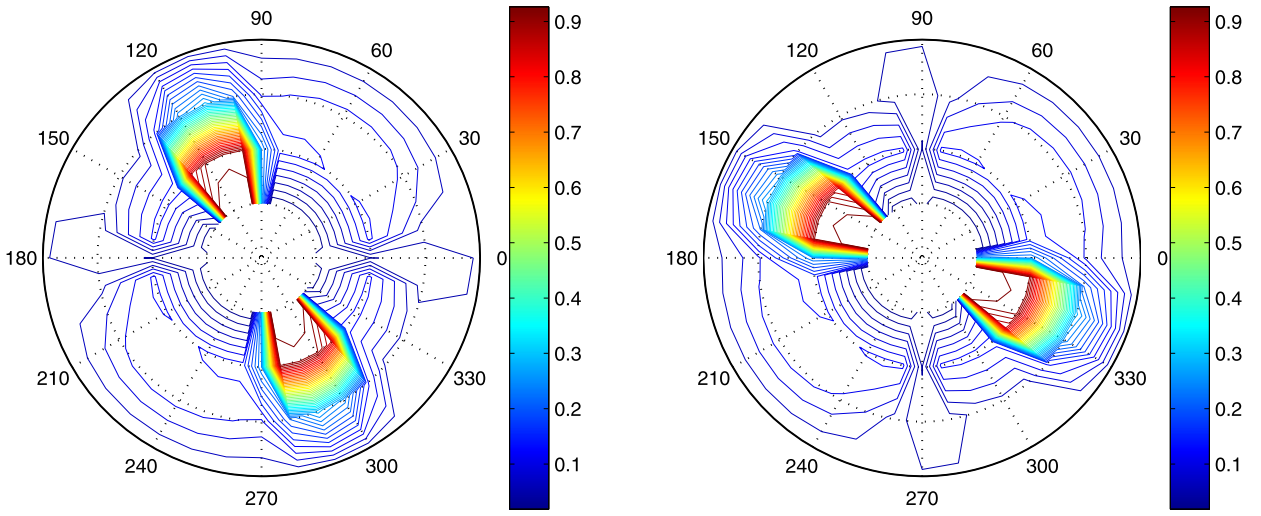

Fig. 10. Three-grid convergence factors predicted by LFA for different values of ε (radial coordinate) and different directions of the anisotropy (angular coordinate) in a right triangular grid, by using a $V(1,1)$-cycle and ILU smoother in the direction (a) west-to-east, south-to-north and (b) south-to-north, east-to-west.

5.1. Oblique flux in a triangular shaped domain

The first numerical experiment deals with the simulation of an oblique flow in an equilateral triangular shaped domain Ω. So, we consider the solution of problem

$$-\nabla \cdot (K \nabla u(\mathbf{x})) = 0, \quad \mathbf{x} \in \Omega, \tag{5.1}$$

$$u(\mathbf{x}) = g(\mathbf{x}), \quad \mathbf{x} \in \partial\Omega, \tag{5.2}$$

where K is the homogeneous anisotropic full-tensor defined in (4.4) with $\varepsilon = 10^{-3}$.

This is a benchmark test for anisotropic diffusion problems, see for example [14]. We are going to analyze the behavior of the proposed ILU based multigrid solver for two different values of angle γ.

In the first test-case, $\gamma = 35°$ and the boundary conditions are chosen such that g is equal to one in a small part of the boundary around vertex $(0,0)$ and zero otherwise. In this way, the flow goes from this vertex to the opposite edge of the triangle in a direction at 35° degrees from the horizontal. We have seen in the previous section (see Fig. 8) that the ILU smoother in the direction west-to-east, south-to-north performs well for this value of angle γ and the shape of the triangular domain. A $V(1,1)$-cycle based on this variant of ILU relaxation is applied to solve the oblique flow problem. In Fig. 11 (a), the history of the convergence of this algorithm for different numbers of refinement levels is displayed. More concretely, we show that around 15 iterations are necessary to reduce the maximum norm of the initial residual in a factor of 10^{-10} for all considered target grids, and therefore the convergence is independent of the space discretization parameter. Also, the obtained numerical solution is presented in Fig. 11 (b), where we can clearly observe the direction of the flow.

In the second test case, we vary the direction of the flow to $\gamma = 135°$ and the boundary conditions are changed in such a way that the non-zero part is now close to vertex $(1,0)$. From results in Section 4.3, we know that the ILU smoother considered in the first test case is not successful anymore in this case and therefore we need to use the one in the direction south-to-north, east-to-west. Based in this smoother, we apply the $V(1,1)$-cycle to solve the problem and in Fig. 12 (a) we display the history of the convergence of the method by showing the reduction of the maximum norm of the residual. In this case, around 13 iterations are enough to obtain the desired convergence, which again is independent on the number of refinement levels. In Fig. 12 (b), the obtained numerical solution in displayed, showing the flow in the considered direction.

5.2. Application to semi-structured grids: L-shaped domain

In the second numerical experiment we consider the solution of the Laplace equation with homogeneous Dirichlet boundary conditions in an L-shaped domain, as the one depicted in Fig. 13. In the multilevel framework, algebraic multigrid is the method most used for the solution of problems in complex domains. However, the application of geometric multigrid that takes advantage of the structure of the grid can be also used for solving these problems by considering a hierarchy of semi-structured triangular grids, see [22]. This hierarchy of grids consists of a completely unstructured coarsest grid and a collection of finer grids obtained by applying successive regular refinements to the initial unstructured grid. In this way,

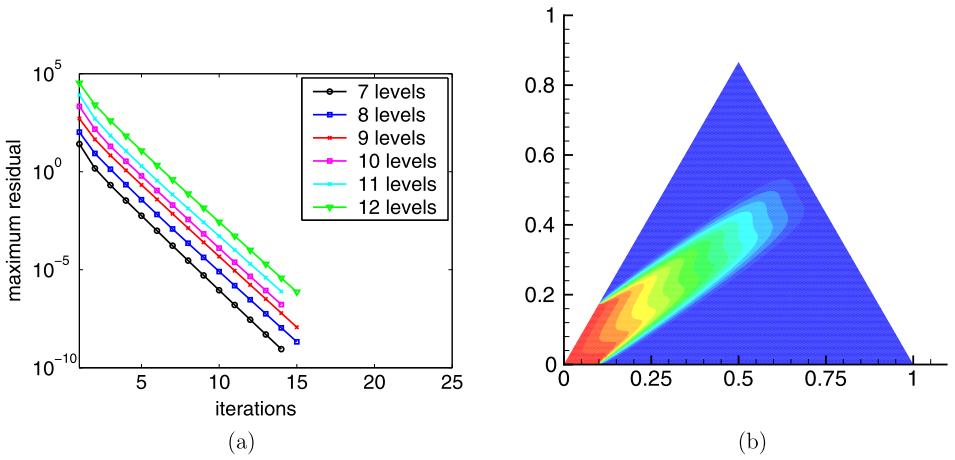

Fig. 11. (a) History of the convergence of a $V(1,1)$-cycle with the ILU_1 smoother in the direction west-to-east, south-to-north, and (b) numerical solution for the oblique flow diffusion problem with angle $\gamma = 35°$.

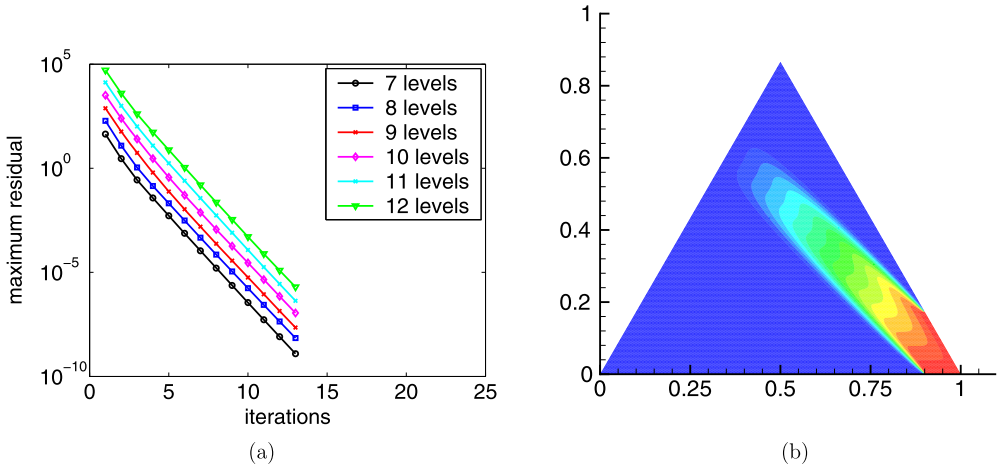

Fig. 12. (a) History of the convergence of a $V(1,1)$-cycle with the ILU smoother in the direction south-to-north, east-to-west, and (b) numerical solution for the oblique flow diffusion problem with angle $\gamma = 135°$.

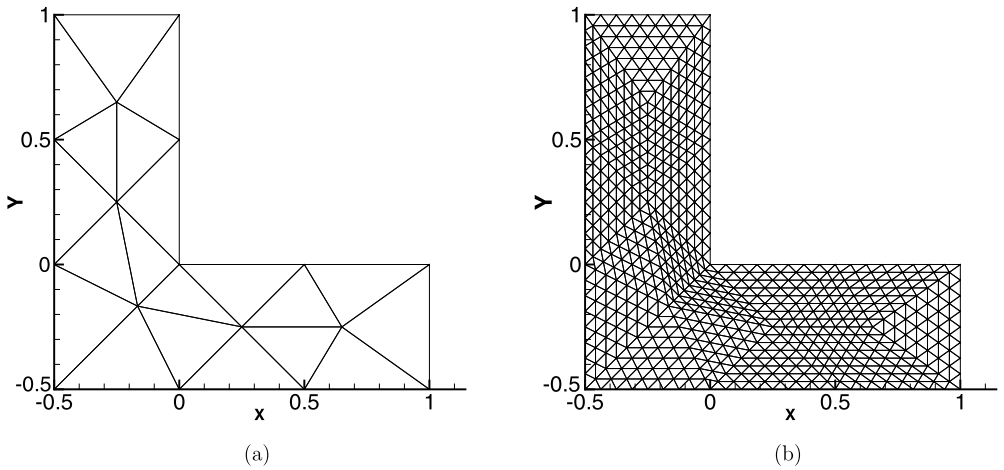

Fig. 13. (a) Coarsest grid for the L-shaped computational domain. (b) Grid in the hierarchy obtained after four refinement levels.

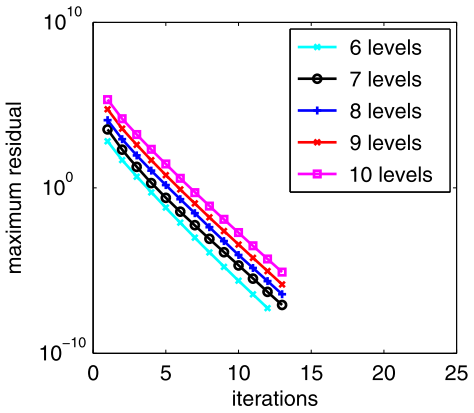

Fig. 14. History of the convergence for different numbers of refinement levels by using a $V(1,1)$-cycle with the ILU smoother in the direction west-to-east, south-to-north.

the target finest grid results in a globally unstructured grid composed by structured patches on which geometric multigrid can be applied. Due to the possibly different geometries on the patches, the multigrid algorithm can be tuned to obtain very good convergence on the resulting different sub-grids. This strategy has been applied in [22], for example, by choosing different components of the algorithm, in particular different smoothers, on each mesh arising on the triangular elements of the coarsest grid. This strategy was shown to be very convenient since the behavior of standard relaxation techniques strongly depends on the geometry of the grid. However, here we do not need to use different smoothers since, as seen in Section 4.1, for this problem, ILU smoother in the direction west-to-east, south-to-north is robust with respect to the geometry of the grid. Therefore, we are going to apply the proposed geometric multigrid, based on this ILU smoother, on a semi-structured triangulation of the L-shaped domain. To construct the hierarchy of meshes, we consider the unstructured coarsest grid shown in Fig. 13 (a) and we apply successively regular refinement. In Fig. 13 (b), we display the grid obtained after four refinement levels, as an example. We apply a V-cycle with one pre- and one post-smoothing steps to solve the problem and the obtained history of the convergence for different numbers of refinement levels is displayed in Fig. 14. In particular, we show the numbers of iterations necessary to reduce the maximum norm of the initial residual in a factor of 10^{-10}. We can see that the convergence is independent on the number of refinement levels and that only 13 iterations are necessary to reach the desired stopping criterion. A global asymptotic convergence factor around 0.17 is obtained, which corresponds to the results shown in Table 2, where the worst factor is around this value. Also, the strategy proposed in [22] can be used here by choosing the other direction of ILU smoother for the triangles on which the convergence is bigger than 0.1. In this case, a global asymptotic convergence factor around 0.11 is obtained by choosing a different ILU ordering in two of the triangles of the coarsest grid.

6. Conclusions

In this work, we have performed a local Fourier analysis to study the smoothing properties of incomplete factorization techniques on triangular grids. This analysis allows us to demonstrate the robustness of a west-to-east, south-to-north ILU smoother which gives very good results for different diffusion problems independently of the geometry of the considered triangular grid. Also, this analysis becomes crucial in the solution of a rotated anisotropic problem on which such ILU smoother is not robust with respect to the changes in the direction of the anisotropy. For this problem, LFA helps us to choose a different direction for the ILU smoother in the way that always one of the two considered orderings provides satisfactory convergence of the multigrid algorithm.

Acknowledgements

The first author is supported by CNPq (Conselho Nacional de Desenvolvimento Científico e Tecnológico, Brazil) scholarship by Science without Borders Program and Federal University of Paraná (Brazil). The work of Francisco J. Gaspar and Carmen Rodrigo is supported in part by the Spanish project FEDER/MCYT MTM2013-40842-P and the DGA (Grupo consolidado PDIE).

References

[1] O. Axelsson, Incomplete block matrix factorization preconditioning methods. The ultimate answer?, J. Comput. Appl. Math. 12 (1985) 3–18.
[2] O. Axelsson, Iterative Solution Methods, Cambridge University Press, New York, NY, USA, 1994.
[3] A. Brandt, Multi-level adaptive solutions to boundary-value problems, Math. Comput. 31 (1977) 333–390.
[4] A. Brandt, Rigorous quantitative analysis of multigrid, I: constant coefficients two-level cycle with l2-norm, SIAM J. Numer. Anal. 31 (1994) 1695–1730.
[5] N.I. Buleev, A numerical method for the solution of two-dimensional and three-dimensional equations of diffusion, Sb. Math. 51 (1960) 227–238.
[6] T.F. Chan, Fourier analysis of relaxed incomplete factorization preconditioners, SIAM J. Sci. Stat. Comput. 12 (1991) 668–680.

[7] T.F. Chan, H.A. van der Vorst, Approximate and incomplete factorizations, in: ICASE/Larc, in: Interdisciplinary Series in Science and Engineering, Kluwer, Dordrecht, 1997, pp. 167–202.
[8] D.J. Evans, The use of pre-conditioning in iterative methods for solving linear equations with symmetric positive definite matrices, IMA J. Appl. Math. 4 (1968) 295–314.
[9] F.J. Gaspar, J.L. Gracia, F.J. Lisbona, Fourier analysis for multigrid methods on triangular grids, SIAM J. Sci. Comput. 31 (2009) 2081–2102.
[10] I. Gustafsson, A class of first order factorization methods, BIT Numer. Math. 18 (1978) 142–156.
[11] W. Hackbusch, Multi-Grid Methods and Applications, Springer, Berlin, 1985.
[12] W. Hackbusch, Iterative Solution of Large Sparse Linear Systems of Equations, Applied Math. Sci. Series, vol. 95, Springer Verlag, 1994.
[13] W. Hackbusch, G. Wittum, Incomplete Decompositions (ILU)-Algorithms, Theory, and Applications, Vieweg+Teubner Verlag, 1993.
[14] R. Herbin, F. Hubert, Benchmark on discretisation schemes for anisotropic diffusion problems on general grids, in: R. Eymard, J.-M. Hérard (Eds.), Finite Volume for Complex Applications, Problems and Perspectives. 5th International Conference, Wiley, London, 2008, pp. 659–692.
[15] K. Johannsen, A robust 9-point ILU smoother for anisotropic problems, IWR Preprint, 2005.
[16] M. Khalil, Local mode smoothing analysis of various incomplete factorization iterative methods, in: W. Hackbusch (Ed.), Robust Multi-grid Methods, in: Notes on Numerical Fluid Mechanics, vol. 23, Vieweg+Teubner Verlag, 1989, pp. 155–164.
[17] J.A. Meijerink, H.A. van der Vorst, An iterative solution method for linear systems of which the coefficient matrix is a symmetric m-matrix, Math. Comput. 31 (1977) 148–162.
[18] K.D. Oertel, K. Stüben, Multigrid with ILU-smoothing: systematic tests and improvements, in: W. Hackbusch (Ed.), Robust Multi-grid Methods, in: Notes on Numerical Fluid Mechanics, vol. 23, Vieweg+Teubner Verlag, 1989, pp. 188–199.
[19] T.A. Oliphant, An implicit numerical method for solving two-dimensional time-dependent diffusion problems, Q. Appl. Math. 19 (1961) 221–229.
[20] T.A. Oliphant, An extrapolation process for solving linear systems, Q. Appl. Math. 20 (1962) 257–267.
[21] G. Rees, D. Silvester, M. Mihajlovic, A truncated ILU smoother for multigrid preconditioning of convection dominated flow problems, MIMS EPrint: 2011.34, Manchester Institute for Mathematical Sciences School of Mathematics, The University of Manchester (April 2011).
[22] C. Rodrigo, F.J. Gaspar, F.J. Lisbona, Geometric Multigrid Methods on Triangular Grids: Application to Semi-Structured Meshes, Lambert Academic Publishing, Saarbrücken, 2012.
[23] R. Stevenson, Modified ILU as a smoother, Numer. Math. 68 (1994) 295–309.
[24] R. Stevenson, Robust multi-grid with 7-point ILU smoothing, in: P. Hemker, P. Wesseling (Eds.), Multigrid Methods IV, in: Int. Ser. Numer. Math., vol. 116, Birkhäuser, Basel, 1994, pp. 295–307.
[25] K. Stüben, U. Trottenberg, Multigrid methods: fundamental algorithms, model problem analysis and applications, in: W. Hackbusch, U. Trottenberg (Eds.), Multigrid Methods, in: Lecture Notes in Mathematics, vol. 960, Springer, Berlin/Heidelberg, 1982, pp. 1–176.
[26] U. Trottenberg, C.W. Oosterlee, A. Schüller, Multigrid, Academic Press, New York, 2001.
[27] N. Umetani, S.P. MacLachlan, C.W. Oosterlee, A multigrid-based shifted Laplacian preconditioner for a fourth-order Helmholtz discretization, Numer. Linear Algebra Appl. 16 (2009) 603–626.
[28] R.S. Varga, Factorization and normalized iterative methods, in: R. Langer (Ed.), Boundary Problems in Differential Equations, Univ. of Wisconsin Press, Madison, 1960, pp. 121–142.
[29] R.S. Varga, Matrix Iterative Analysis, Prentice-Hall Inc., Englewood Cliffs, NJ, 1962.
[30] P. Wesseling, Theoretical and practical aspects of a multigrid method, SIAM J. Sci. Stat. Comput. 3 (1982) 387–407.
[31] P. Wesseling, An Introduction to Multigrid Methods, John Wiley, Chichester, UK, 1992.
[32] P. Wesseling, P. Sonneveld, Numerical experiments with a multiple grid and a preconditioned Lanczos type method, in: R. Rautmann (Ed.), Approximation Methods for Navier–Stokes Problems, in: Lecture Notes in Mathematics, vol. 771, Springer, Berlin/Heidelberg, 1980, pp. 543–562.
[33] R. Wienands, W. Joppich, Practical Fourier Analysis for Multigrid Methods, Chapman and Hall/CRC Press, 2005.
[34] R. Wienands, C.W. Oosterlee, On three-grid Fourier analysis for multigrid, SIAM J. Sci. Comput. 23 (2001) 651–671.
[35] G. Wittum, Linear iterations as smoothers in multigrid methods: theory with applications to incomplete decompositions, Impact Comput. Sci. Eng. 1 (1989) 180–215.
[36] G. Wittum, On the robustness of ILU smoothing, SIAM J. Sci. Stat. Comput. 10 (1989) 699–717.